Microfluidics and Nanofluidics (2024) 28:24
https://doi.org/10.1007/s10404-024-02718-y

RESEARCH

Behaviors of non-wetting phase snap-off events in two-phase flow: microscopic phenomena and macroscopic effects

Ran Li[1,2] · Zhaolin Gu[1] · Zhang Li[3] · Weizhen Lu[2] · Guozhu Zhao[4] · Junwei Su[1]

Received: 14 September 2023 / Accepted: 13 February 2024 / Published online: 26 March 2024

Abstract

Snap-off events are one of the most common and essential phenomena in two-phase flow in porous media. This paper uses the scanning results of a siltstone slice to construct a two-dimensional heterogeneous pore network structure to visualise microscopic snap-off phenomena and displacement processes accurately. The relationship between snap-off events and the non-wetting phase saturation was studied using two-phase flow displacement experiments. Results show that although the non-wetting phase snap-off events benefit freeing the trapped non-wetting phase in the microchannels, high-frequency snap-off events are the main reason for trapping the non-wetting phase during the displacement process, eventually leading to residuals. The frequency of non-wetting phase snap-off events in the pore network structure can be reduced to lower the non-wetting phase saturation and reduce the non-wetting phase residuals by increasing the displacement fluid viscosity, reducing the surface tension coefficient between the phases and increasing the flow rate.

Keywords Snap-off · Two-phase flow · Pore network · Viscosity ratio · Residuals mobilisation · Capillary number

1 Introduction

Porous media comprises interconnected three-dimensional pore space networks with varying sizes and shapes with a particular porosity and high specific surface area (Ghanbarian et al. 2013). Crude oils are usually trapped in porous geological media as oil droplets, films, and ganglions (Perazzo et al. 2018). On a microscopic scale, the development of secondary oil recovery involves primarily multi-phase flows in porous media, and water flooding creates an emulsion inside the reservoir, allowing oil to flow through the structure (Pak et al. 2015). Formation analyses and mobilisation regimes of the residual oil remaining in the porous media after water flooding are essential research subjects for secondary oil recovery (Perazzo et al. 2018; Singh et al. 2019; Alhosani et al. 2020).

Water is usually injected into the reservoir during flooding to drive oil from the pore spaces. However, because of the small throat, pore sizes, and fluid with high viscosity, the porous medium flow can be severely suppressed regardless of the injection pressure. In addition, high water–oil interfacial tension and wettability (e.g., oil firmly attached to rocks) inhibit oil displacement (Buchgraber et al. 2012; Joekar-Niasar and Hassanizadeh 2012; Esmaeili et al. 2020). Many residuals are distributed in the pores and throats after water flooding, which may cause the non-wetting phase to be trapped in the porous medium (Datta et al. 2014; Pak et al. 2015). In the imbibition and drainage displacement process, oil phase snap-off is one of the leading causes of trapped residual oil, and the release of the remaining oil in the microchannels is also closely related to this microscopic event (Datta et al. 2014; Singh et al. 2019).

Pore-scale droplet snap-off phenomena exist widely in various natural and industrial engineering flow processes, such as crude oil exploitation (Yun and Kovscek 2015), carbon dioxide geological storage (Riazi et al. 2011), and

✉ Guozhu Zhao
zhaoguozhu@cardc.cn

✉ Junwei Su
sujunwei@mail.xjtu.edu.cn

1 School of Human Settlements and Civil Engineering, Xi'an Jiaotong University, Xi'an 710049, China

2 Department of Architecture and Civil Engineering, City University of Hong Kong, Hong Kong, China

3 Wuxi Environmental Monitoring Center, Wuxi 214026, China

4 Science and Technology on Scramjet Laboratory, China Aerodynamics Research and Development Center, Mianyang, China

emulsification (Esmaeili et al. 2020). The droplet snap-off process crucially influences the behavior of multi-phase fluids in porous media (Singh et al. 2019). When the non-wetting phase displaces the wetting phase in a microchannel, the wetting phase forms a wetting film on the channel wall (Roman et al. 2017). Snap-off occurs when the wetting phase, under capillary pressure, accumulates in a pore throat occupied by the non-wetting phase and then bridges across the throat to block the flow (Rossen 2000). The non-wetting phase breaks up and generates tiny non-wetting phase droplets.

In the single pore-throat model, Li et al. (Li et al. 2021, 2022) explained the physical mechanism of the non-wetting phase snap-off event, provided the criteria for judging its occurrence, and analyzed the physical parameters affecting it. Other researchers have revealed the flow mechanisms in porous media by focusing on various topics, including fluids displacement in capillary ducts (Lenormand et al. 1983), oil–water interface changes (Ayirala et al. 2018; Li et al. 2019), oil–water pathway distribution (Chen et al. 2005; Liang et al. 2020), the influence of pore geometry parameters (Buchgraber et al. 2012; Singh et al. 2016; Xu et al. 2017; Yun et al. 2017; Osei-Bonsu et al. 2018; Alhosani et al. 2020), the effect of displacement fluid on oil recovery (Mahdavi and James 2019), relative permeability (Berg et al. 2016), and 3D imaging of pore-scale processes (Pak et al. 2015; Singh et al. 2017). Blunt (Blunt 1998) proposed an intermediate-wet porous media model to analyze the influence of wettability on residual oil saturation, showing that residual oil saturation varies significantly with wettability over a wide range for a model with a fixed pore and throat size distribution. For example, residual oil saturation varied between 5 and 50% as the oil-wet pore fraction was altered. Snap-off was the dominant oil-trapping mechanism in porous media. An increased contact angle caused the snap-off event to become less favored, and the residual oil saturation decreased. Ruspini et al. (Ruspini et al. 2017) proposed a new cooperative pore-body filling model to study the capillary trap phenomenon in water-wet porous media. Their model demonstrated that the number and distribution of non-wetting phase traps are determined by the competition between snap-off and cooperative pore-body filling trap mechanisms, which can be used to predict residual non-wetting phase saturation and capillary capture curves. The measured contact angle indicated the capillary pressure scanning curve and the relative permeability of sandstone, in good agreement with experimental results. Alyafei et al. (Alyafei and Blunt 2016) studied capillary trap events in cores with different wettabilities and the effects of trap events on residual oil saturation with displacement experiments. The capillary trap phenomenon under water-wet conditions was principally caused at the pore scale by snap-off, with little oil production after water breakthrough (Hammond 1983). Water filled the narrowest part of the pore space during water flooding, while oil remained in the larger pores, resulting in a sizeable residual oil saturation. As the initial oil saturation increased, more oil could be trapped, increasing residual oil saturation. In summary, previous research on snap-off events in porous media has mainly focused on capturing the snap-off phenomenon and its effect on the capillary trap phenomenon rather than its occurrence and influence on downstream fluids. There are many microscopic phenomena in the porous media displacement process, making it difficult to determine the effect of a single phenomenon on the displacement process using traditional displacement experiments.

The rapid development of microfluidic technology permits studying the microscopic snap-off process and its influence on the macroscopic flow field with greater visualization capability and high fluid control precision. Changing the displacement conditions and fluid properties can reveal the influence of non-wetting phase fluid snap-off events on the two-phase flow for different flow conditions. Based on two-phase fluid displacement experimental results in porous media, the change in non-wetting phase saturation caused by the snap-off events may be quantified. To our knowledge, few studies have quantified the non-wetting phase saturation change caused by non-wetting phase fluid snap-off events during two-phase flow.

In this paper, we obtained a pore structure network from the scanning results of a siltstone slice and processed a silicon wafer mold using soft lithography (Rogers and Nuzzo 2005). We then fabricated a full PDMS (polydimethylsiloxane) microfluidic chip with a pore network structure that can characterize the microchannel structure in real rock cores. This microfluidic chip was used to conduct two-phase fluid displacement experiments to study the influence of non-wetting phase fluid snap-off events on the two-phase flow. Analyzing the microscopic phenomena caused by snap-off events, summarizing the non-wetting phase snap-off regime in the pore network structure, and revealing the residual distribution of the non-wetting phase in the pore network structure was shown to be effective in reducing the saturation of the pore network structure non-wetting phase.

2 Materials and methods

2.1 Pore network structure chips and reagents

As shown in Fig. 1, microfluidic chips with a two-dimensional heterogeneous pore network structure were used in the displacement experiment. Figure 1a shows the pore network structure model derived from the siltstone slice scanning results. C1 and C2 are the wetting and non-wetting phase fluid inlets, respectively, and C3 is the mixture outlet. In

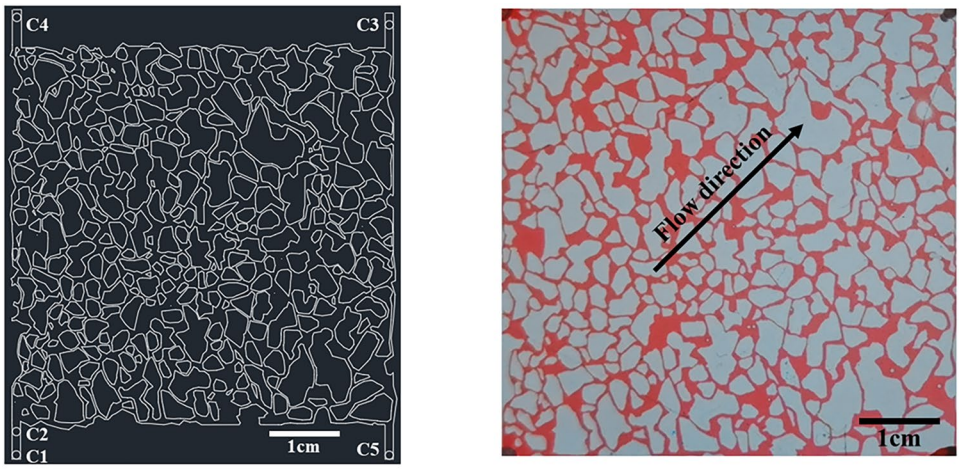

Fig. 1 The microfluidic chip used in experiments. **a** Two-dimensional heterogeneous pore network structure model. C1 and C2 are the wetting and non-wetting phase fluid inlets, respectively. C3 is the mixture outlet, and C4 and C5 are the inlets for cleaning chips. **b** PDMS chip saturated with wet phase fluid. The red part shows the microchannels saturated with wetting phase fluid, and the white part shows the PDMS substrates

the displacement experiment, the central axis of the flow direction is along the diagonal direction of the pore network structure. C4 and C5 are the cleaning chip inlets used for cleaning processes and wetting phase saturation operations.

The PDMS base (SYLGARD 184 Silicone Elastomer Kit Base, Dow Corning) was mixed with a curing agent at a 10:1 ratio and defoamed in a vacuum chamber. Then, the mixture was coated on the silicon wafer mold and heated in an oven at 85 ℃ for 30 min to cure the liquid PDMS. The same operation was carried out to prepare the PDMS layer without channels on a single polished wafer mold, which was used to compose an entire PDMS chip. After cooling and demolding, the PDMS samples were placed in a plasma cleaner (Harrick. PDC-002 Plasma Cleaner, USA) and treated for 50 s with oxygen plasma for surface activation.

Finally, the two PDMS layers were bonded and baked above 65 ℃ for 24 h to ensure the microchannels' hydrophobicity (Jin et al. 2010). The contact angles between mineral oil (with 3 wt% Span-80) and PDMS layer was 33.5°, the contact angles between deionized water, 30 wt% glycerol aqueous solution, 65 wt% glycerol aqueous solution, and 85 wt% glycerol aqueous solution with PDMS layer were 91°, 104.3°, 100°, and 103.8°, respectively. Figure 1b shows a PDMS chip saturated with wetting phase fluid. The microfluidic chip was etched with a complex pore network structure, including micro-channel structures with different widths and directions, complex micro-channel inlet and outlet structures, pore structures, and throat structures of various sizes. The red part shows the microchannels filled with wet phase fluid, and the white part shows the PDMS substrates.

Residual oil saturation is the volume percentage of crude oil remaining in the rock pores that cannot be recovered after several displacement processes (Mehmani et al. 2019; Heydari-Farsani et al. 2020; Song and Hatzignatiou 2022). After multiple displacement processes, the oil phase remains in the water-wet porous media as non-wetting phase residuals. In these displacement experiments, the non-wetting phase saturation in the pore network structure characterized the residual oil saturation. Mineral oil dyed with an oil-soluble red was used as the wetting-phase fluid, and different mass fraction aqueous glycerol solutions stained with methyl blue were used as the non-wetting phase fluid. Fluid parameters are shown in Table 1. The two-phase viscosity ratio $k = \mu_{NW}/\mu_W$ was varied from 0.08 to 10.44 by adjusting the glycerol solution viscosity.

In the displacement experiments, glycerol aqueous solutions with different mass fractions and mineral oil simulated the two-phase fluid with different viscosity ratios (Table 1). The displacement process of the non-wetting phase liquid group under different flow conditions and the change in

Table 1 Physical properties of the experimental fluids (25 ℃)

Materials number	Wetting phase	μ_W(mPa·s)	Non-wetting phase	μ_{NW}(mPa·s)	Interfacial tension coefficient (mN·m^{-1})
M1	3 wt% Span 80 + mineral oil	12.57	Deionised water	1	4.76
M2	3 wt% Span 80 + mineral oil	12.57	30 wt% glycerol aqueous solution	2.77	8.43
M3	3 wt% Span 80 + mineral oil	12.57	65 wt% glycerol aqueous solution	13.41	10.21
M4	3 wt% Span 80 + mineral oil	12.57	85 wt% glycerol aqueous solution	131.21	10.71

non-wetting phase saturation caused by snap-off events were then analyzed.

2.2 Experimental setup and procedures

Figure 2 shows the displacement experiment platform. Syringe pumps (CETONI neMESYS Middle Pressure Module,

Germany) injected fluids into the microfluidic chip. A high-resolution camera matrix (Teledyne Dalsa Genie Nano-CL M2420, Canada) recorded the flow phenomena, achieving a high frame rate (30 fps) and high-resolution image recording (10^8 pixels per frame) to capture microscopic phenomena and macroscopic flow trends occurring during the flow process.

The non-wetting phase fluid displacement experimental procedure is as follows. First, two-phase fluids are injected into the pore network structure to expel the air in the tubes between the syringe pump and the chip. Then, the non-wetting phase fluid injection is stopped, and the wetting phase fluid is continuously injected into the chip at a constant flow rate until it saturates the entire pore network structure. Next, the non-wetting phase fluid is injected into the chip at a specified flow rate until it flows to the chip outlet to form a non-wetting phase fluid pathway. The time t_{io}, from the initial non-wetting phase fluid injection to the flow reaching the chip outlet, is recorded.

The non-wetting phase fluid injection is then stopped, and the wet-phase fluid is continuously injected into the chip at the same flow rate (the sum of the wetting phase fluid rate and non-wetting phase fluid rate at t_{io}) for a duration of 5 times t_{io}. At this time, the injection of two-phase fluids is stopped. The non-wetting phase residual in the pore network structure is considered the final residual after the displacement process. The non-wetting phase saturation is calculated from the two-phase distribution.

3 Results

Experimental results for a two-phase fluid displacement experiment with material M2 at an inlet capillary number $Ca \approx 10^{-3}$ ($Ca = \mu_W U/\sigma$, where μ_W is the wetting phase viscosity, U is the inlet fluid velocity, and σ is the interfacial tension coefficient of the two phases. $U = (Q_W + Q_{NW})/S_{IN}$, where S_{IN} is the inlet cross-section area, Q_W and Q_{NW} are the injection flow rate of the wetting phase and non-wetting phase, respectively.) are shown in Fig. 3. The pore network structure reached the wetting phase saturation at an injection flow rate of 20 μL/min. The flow direction was along the microfluidic chip's diagonal path.

As shown in Fig. 3a, the microfluidic chip was wetting-phase-saturated at T = 0 s, and the non-wetting phase fluid injection into the chip started at a 10 μL/min flow rate. At T = 15 s, the non-wetting phase fluid integrally diffused along the flow direction Fig. 3b. Because there was a pore-throat structure with a large pore-throat ratio in the flow direction, a considerable breakthrough pressure (Rezaei et al. 2018; Cui et al. 2022; Zhang and Wang 2022) was required to allow the non-wetting phase fluid to invade the

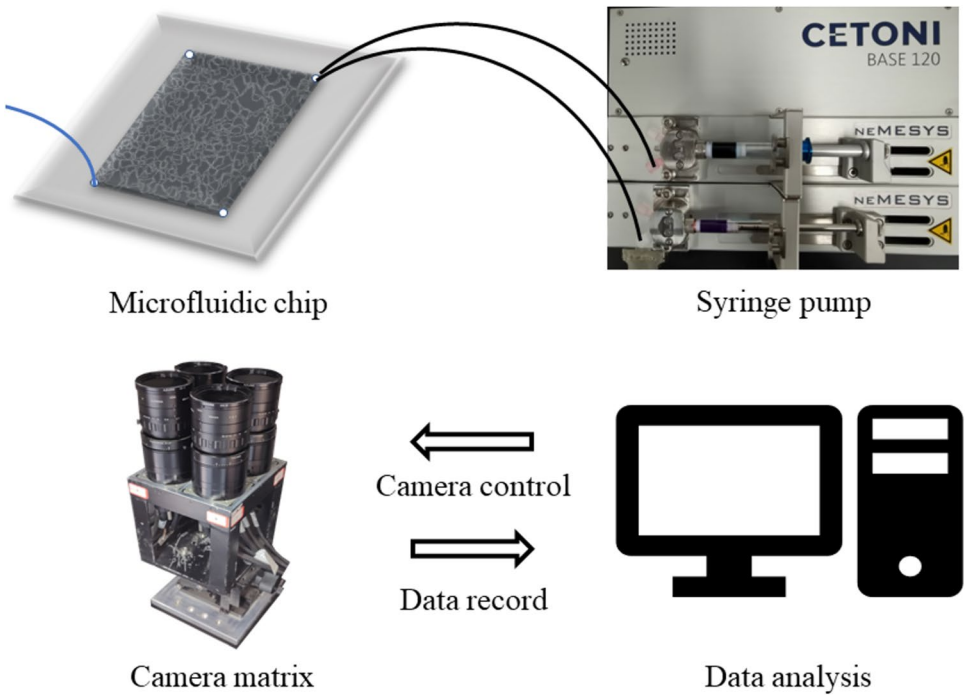

Fig. 2 A microfluidic experimental system for visualizing flow phenomena

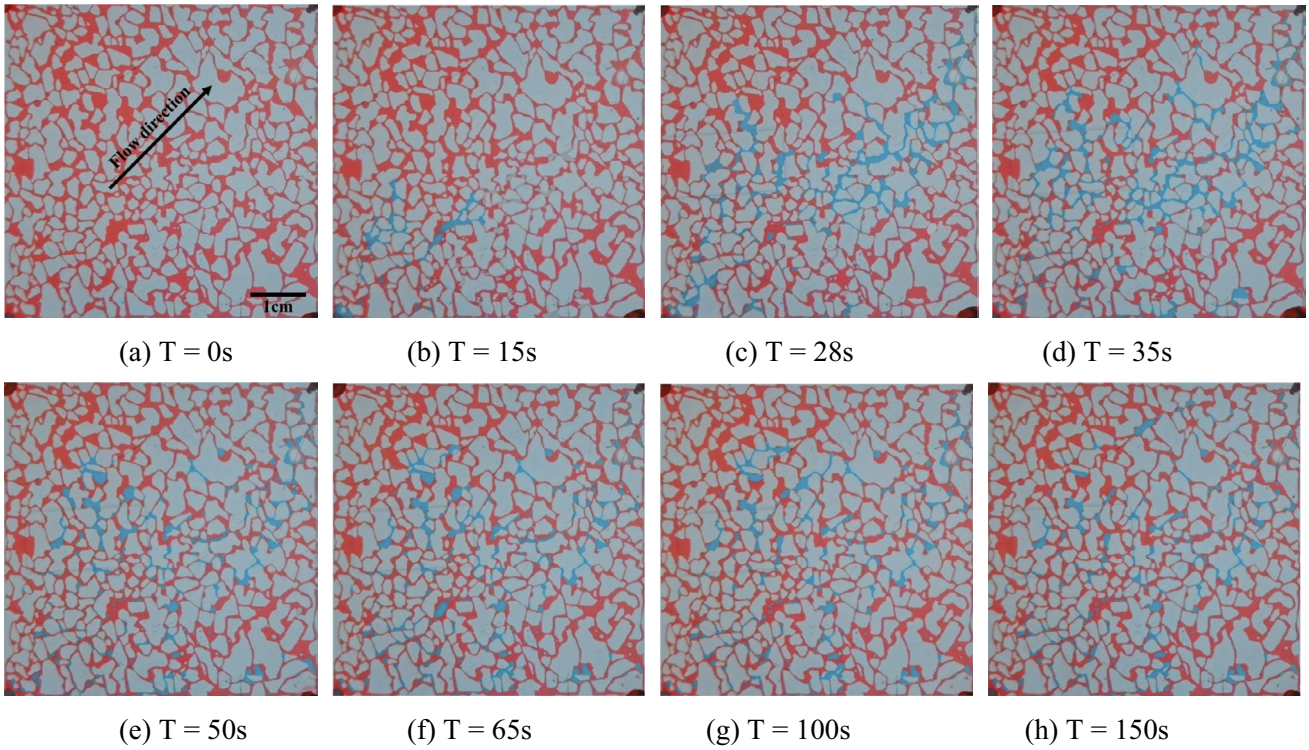

Fig. 3 Diagram of two-phase fluid distribution in displacement experiment. **a**–**h** are two-phase fluid distribution diagrams at different times. The red part represents the wetting phase fluid, and the blue region represents the non-wetting phase fluid. The injection flow rate of the wetting phase and non-wetting phase were 20μL/min and 10μL/min, respectively. Material M2 was used in the experiment, and the inlet capillary number was $Ca = 0.0018$

microchannel downstream of the pore-throat structure, and the non-wetting phase fluid simultaneously diffused along the flow's axial direction.

At T = 28 s, the non-wetting phase fluid reached the mixture outlet along the flow direction, and a non-wetting phase pathway was formed Fig. 3c. The non-wetting phase fluid injection was stopped, and the wetting phase fluid continued to be injected into the chip at a 20 μL/min flow rate. At T = 35 s, while the wetting phase fluid was injected, the non-wetting phase fluid snapped and formed discontinuous liquid ganglions Fig. 3d.

When the snap-off events occurred, non-wetting phase fluid accumulated within the pore structures along the direction with less flow resistance. Figure 3e–g shows that the wetting phase fluid gradually formed a wetting phase pathway along the flow direction with the wetting phase fluid injection. During the wetting phase pathway formation, the snapping frequency of the non-wetting phase fluids gradually decreased, and the area farther from the axial flow direction could no longer be affected by the injected wetting phase fluid. The non-wetting phase liquid ganglions from the axial direction gradually trapped upstream of the pore-throat structure and within the pore structure, no longer moving in the subsequent flow process. Meanwhile, the residual non-wetting phase fluid ganglions along the flow direction continued to snap off, generating smaller droplets that flow to the microfluidic chip outlet.

At T = 150 s, non-wetting phase fluid could not be released and flowed to the outlet Fig. 3h. The non-wetting phase fluid remaining in the pore network structure was considered the non-wetting phase residual.

Figure 4 describes the two-phase fluid saturation change in the displacement experiment. The pore network structure was initially saturated with the wetting phase fluid. The wetting phase saturation decreased with the injection of the non-wetting phase fluid, and the non-wetting phase saturation reached its maximum when it formed a pathway along the flow direction. The non-wetting phase saturation was about 21% at T = 28 s.

When the injection of non-wetting phase fluid stopped, the saturation gradually decreased during the wetting phase injection, reaching 10.8% at the end of the displacement experiment and changing slightly from T = 100 s to T = 150 s. The non-wetting phase liquid ganglions cannot be moved in the subsequent flow process because they are trapped during displacement.

This experiment simulated the residual oil release in the water-wet reservoir core with high water saturation. It was

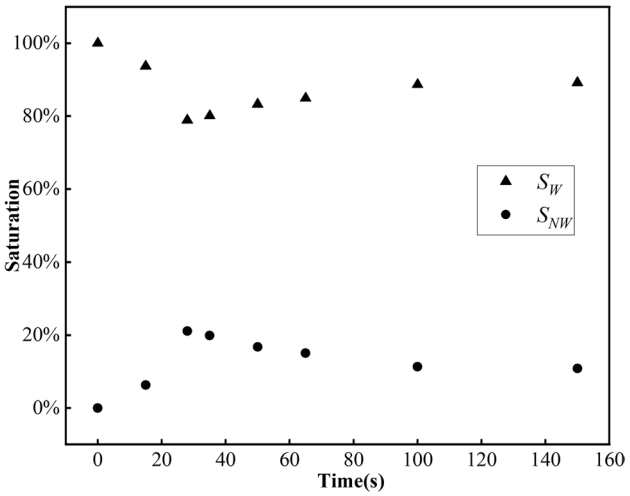

Fig. 4 Two-phase fluid saturation changes in displacement experiments. The experiment was set up with materials M2 at $Ca = 0.0018$, and percolation started at T = 0 s. The triangles and circles symbols represent the saturation of wetting and non-wetting phases, respectively

found that the non-wetting phase residuals snapped in the pore throat structure and became trapped again in the pore structure along the flow direction when migrating along that direction. Non-wetting phase residuals formed, which are difficult to move.

4 Discussion

4.1 Snap-off behavior in the pore throat structure

The non-wetting phase fluid ganglion displacement experiment showed that the snap-off event was the main reason for the trapped non-wetting phase fluid. As shown in Fig. 5, a non-wetting phase droplet flowed upstream of a pore-throat structure at T = 40 s. The droplet broke to form two smaller, non-wetting phase daughter droplets at T = 48 s when it flowed through a microchannel with a narrow constriction. At T = 150 s, after a long injection period, the non-wetting phase droplets remained in the pore structure, forming trapped non-wetting phase droplets.

Although the wetting phase fluid was still injected during the droplet trapping process, the local flow field could no longer reach the snap-off condition for the non-wetting phase droplets, and the wetting phase fluid flowed to the outlet along the formed pathway. The non-wetting phase fluid snap-off event caused the non-wetting phase droplets and ganglions to form and was the reason for the trapping of non-wetting phase fluid. Figure 5c shows that non-wetting phase daughter droplets generated by the snap-off event were trapped in the pore throat structure. Daughter droplet 1 elongated along the flow direction, but the driving force on the daughter droplet at these flow conditions could not overcome the capillary pressure at the front of the droplet, so it could not enter the downstream pore throat structure. Daughter droplet 2 was trapped in the pore structure, and the droplet's driving force could not overcome the capillary pressure of the droplet, so this droplet could not be mobilised in the flow process. Frequent snap-off events of the non-wetting phase liquid ganglions during the flow process, while non-wetting phase droplets separated from the liquid ganglions were trapped in the pore throat structure during the flow process. The trapped non-wetting phase liquid droplets and ganglions increased the local flow resistance (Rossen 2000; Beresnev et al. 2009; Peña et al. 2009; Datta et al. 2014), making it more difficult to release the trapped non-wetting phase fluid in the pore throat structure, finally leading to increased non-wetting phase saturation in the pore network.

Meanwhile, the snap-off event also caused the movement of the trapped non-wetting phase in the pore throat structure. Figure 6 traces the direction of the trapped non-wetting phase in the wetting phase fluid displacement experiment. At T = 24 s, the trapped non-wetting phase droplet in the pore structure elongated along the flow direction and reached the upstream part of the throat. At T = 38 s, the non-wetting phase droplet continuously snapped off at the throat to form tiny daughter droplets that flow out of the pore throat structure along the flow direction. At T = 47 s, the trapped non-wetting phase in the pore structure was fully released, and there was no remaining fluid in the pore structure.

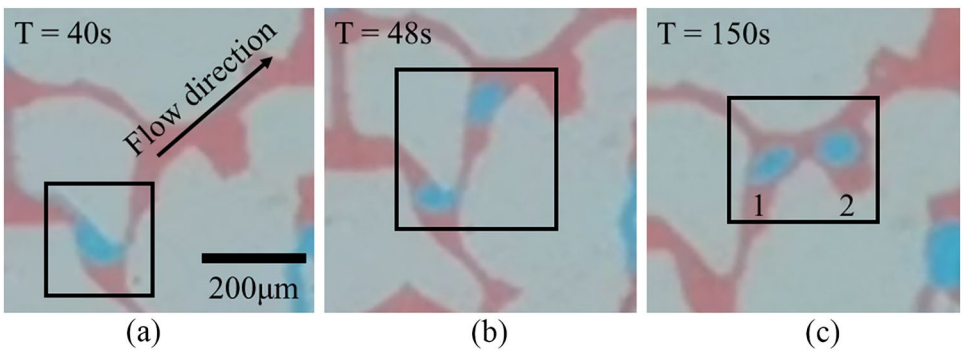

Fig. 5 Diagrams of non-wetting phase droplet trapping process in the pore throat structure. **a**–**c** are the time series of the trapping process. Material M2 was used in the experiment, and the inlet capillary number was $Ca = 0.0018$. The red and blue parts represent the wetting and non-wetting phases of fluid, respectively

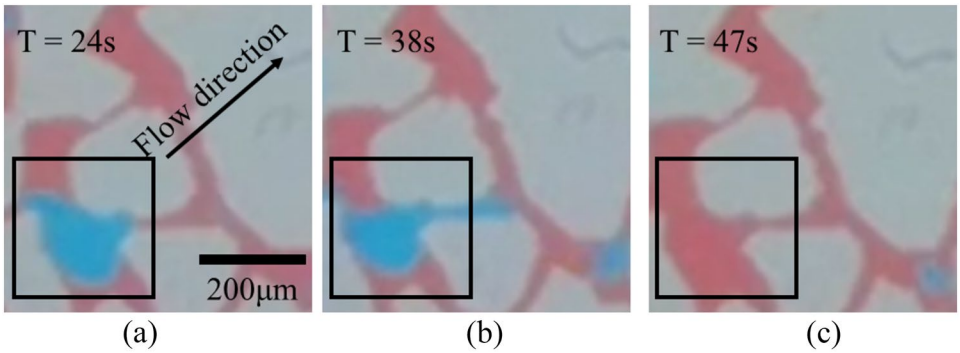

Fig. 6 Diagrams of the trapped non-wetting phase droplet mobilising process in pore throat structure. **a**–**c** are the time series of the trapping process. Material M2 was used in the experiment, and the inlet capillary number was Ca = 0.0018. The red and blue parts represent the wetting and non-wetting phases of fluid, respectively

A comparison of the different phenomena in Figs. 5 and 6 shows that although the snap-off events are beneficial in freeing the trapped non-wetting phase in the pore throat structure, snap-off events are the main reason for the trapping of the non-wetting phase during the displacement process, eventually leading to the residuals. The non-wetting phase snap-off events in a single pore affect only the local flow field. Still, variations in the snap-off frequency change the non-wetting phase distribution in the pore network, and the aggregation of microscopic events eventually has a macroscopic impact.

4.2 Non-wetting phase snap-off tendencies in the pore network structure

One of the most common phenomena in oil recovery is oil droplet snap-off, which occurs during water injection in water-wet porous media (Garstecki et al. 2005; Cubaud and Mason 2008; Beresnev et al. 2009; Andrew et al. 2015; Singh et al. 2017). The oil droplets are eventually trapped in the pores, creating a significant loss. The number of non-wetting phase droplets representing the snap-off frequency was continuously recorded during the displacement experiment to compare the differences in the snap-off for different flow rates and two-phase viscosity ratios.

As shown in Fig. 7, the non-wetting phase fluid in the pore network structure exhibited different snap-off tendencies at different inlet capillary numbers. At lower inlet capillary numbers, the frequency of non-wetting phase snap-off events was higher, and more non-wetting phase droplets were formed. At an inlet capillary number $Ca \approx 10^{-3}$($Ca = 0.0018$), droplets formed by non-wetting phase snap-off events increased with the injection of wetting phase fluids, and more non-wetting phase droplets remained in the pore network after the displacement process. The increasing number of non-wetting phase droplets indicates that the non-wetting phase snap-off event was the primary mechanism of non-wetting phase trapping for this inlet flow condition.

With an increase in the flow rate, the inlet capillary number reached $Ca \approx 10^{-2}$($Ca = 0.017$), and the number

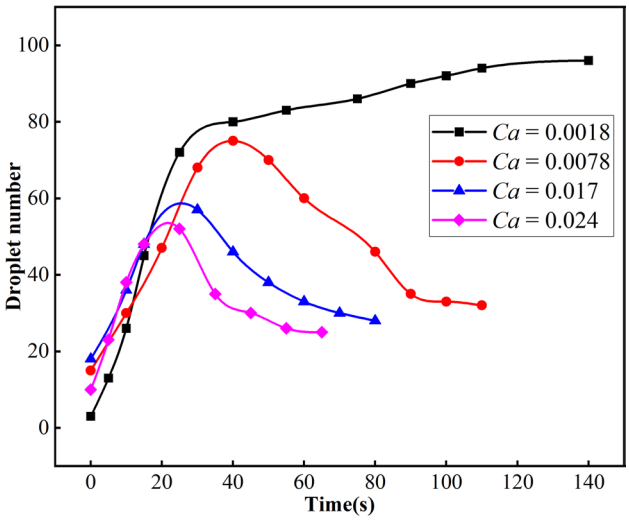

Fig. 7 Diagram of non-wetting phase droplets number at different inlet capillary numbers. The experiment was set up with materials M9, and all percolation processes started at T = 0 s

of non-wetting droplets first increased and then decreased. Non-wetting phase snap-off events can release the non-wetting phase fluids trapped in the pore throat to a certain degree, but they are the primary mechanism causing non-wetting phase residuals in the pore network. For example, non-wetting phase fluids snapped to form 75 droplets in the pore network structure at inlet $Ca = 0.0078$ at T = 40 s. Subsequently, the occurrence of the non-wetting phase snap-off events and the number of droplets in the pore network structure gradually decreased. Only 32 non-wetting phase droplets remained in the pore network structure at the end of the displacement process. The change in the number of non-wetting phase droplets indicates that droplets generated by non-wetting phase fluid snap-off events later reduce the non-wetting phase residuals in the pore network structure.

The number of droplets generated by non-wetting phase fluid snap-off events was further decreased as the inlet capillary number increased, and the non-wetting phase residuals in the pore network structure were also reduced after

the displacement process. When $Ca > 10^{-2}$, the changes in the numbers of non-wetting phase droplets initially increased, followed by a decreasing trend.

As shown in Fig. 8, non-wetting phase fluids had different snap-off tendencies for different two-phase viscosity ratios. In Fig. 8a, at inlet $Ca \approx 10^{-3}$($Ca = 0.0018$), non-wetting phase fluids snapped and generated droplets with the injection of wetting phase fluids, gradually increasing and remaining in the pore network structure after the displacement process. The larger the viscosity ratio of the two phases, the fewer non-wetting phase droplets were generated during the displacement process. It was consistent with the effect of viscosity on the droplet breakup process obtained in single pore throat experiments (Peña et al. 2009; Li et al. 2021, 2022), i.e., high viscosity non-wetting phase fluids were more challenging to snap off.

In Fig. 8b, non-wetting phase fluids showed the same snap-off trends for different two-phase viscosity ratios at inlet $Ca \approx 10^{-2}$($Ca = 0.017$). The number of droplets generated by non-wetting phase fluid snap-off events showed a trend that first increased and then decreased. Non-wetting phase fluids continuously snapped and generated dispersed droplets that entered the microchannels and pore throat structures along the minimum dynamic pressure drop direction. Some droplets continued to break and flowed out of the pore network structure along the flow direction. The remaining droplets were trapped in the pore network structure, resulting in non-wetting phase residuals.

4.3 Residual distributions of non-wetting phase fluids in the pore network structure

The displacement experiments demonstrated that the non-wetting phase snap-off tendencies were different for different inlet capillary numbers and viscosity ratios of the two phases, ultimately resulting in different non-wetting phase residual distributions in the pore network structure. The distribution tendencies of non-wetting phase residuals and the influence of non-wetting phase snap-off events on non-wetting phase saturation in the pore network structure were studied by recording the final numbers and areas of non-wetting phase droplets remaining in the pore network structure for different displacement conditions. This information assists in finding an effective method to reduce non-wetting phase saturation as much as possible by adjusting the snap-off frequency.

Figure 9a shows the distribution of non-wetting phase residuals for different inlet capillary numbers. Non-wetting phase fluids snapped and generated more droplets at low capillary numbers. More than half of the non-wetting phase droplets had areas between 2×10^6 μm^2 and 4×10^6 μm^2, and the other non-wetting phase droplets had areas between 4×10^6 μm^2 and 22×10^6μm^2. As the inlet capillary number increased, the number of droplets decreased, but the area distribution of non-wetting phase droplets changed slightly. More than half of the droplets are small-volume, non-wetting phase droplets and the rest are dispersed with areas in the range of 4×10^6 μm^2 to 22×10^6μm^2.

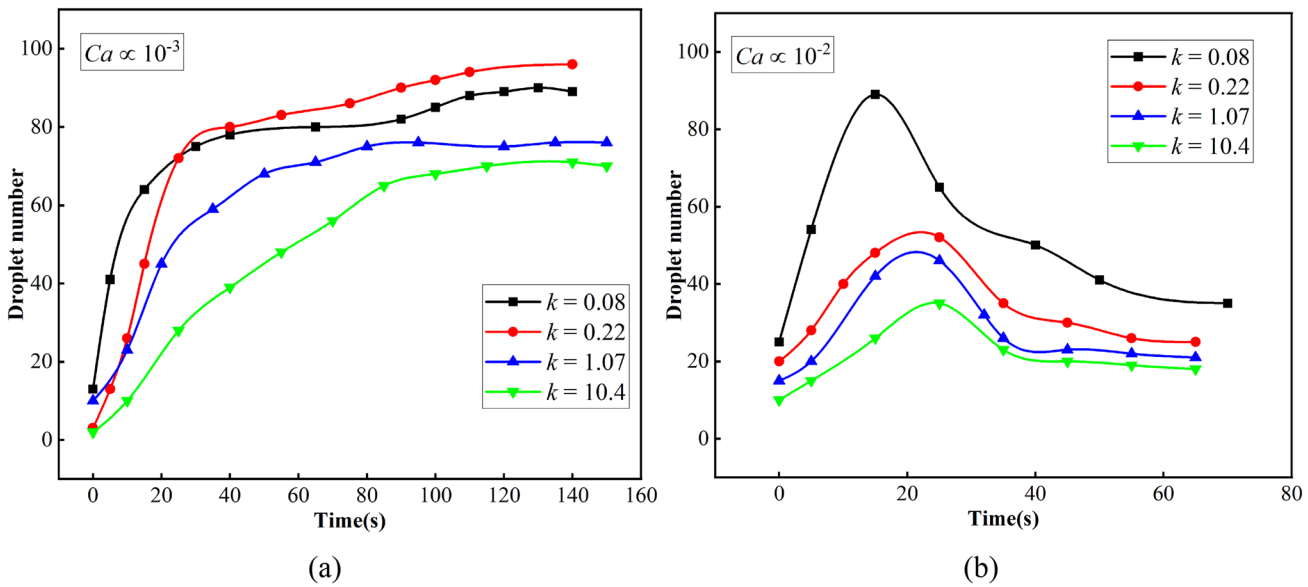

Fig. 8 Diagrams of non-wetting phase droplets number for different two-phase viscosity ratios. The experiment was set up with materials M1-M4, and all percolation processes started at T = 0 s. **a** and **b** show the different non-wetting phase droplet numbers at inlet $Ca \approx 10^{-3}$($Ca = 0.0018$) and $Ca \approx 10^{-2}$($Ca = 0.017$), respectively

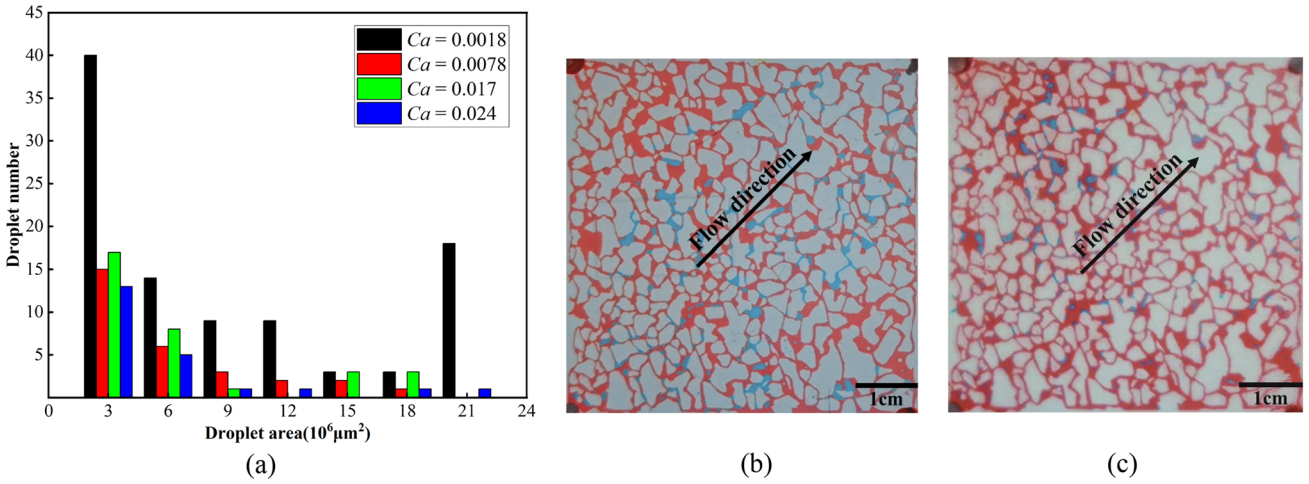

Fig. 9 Distribution diagrams of the non-wetting phase residuals in the displacement experiment. **a** is a statistical diagram of the residual droplets in the non-wetting phase at different inlet capillary numbers. Experiments were set up with materials M2. **b** and **c** are the experimental diagram of the non-wetting phase residual distribution at inlet $Ca = 0.0018$ and $Ca = 0.024$, respectively. The red, blue and white parts represent the wetting phase fluid, non-wetting phase fluid and the PDMS substrates, respectively

Figure 9b shows the non-wetting phase residual distribution diagram for inlet $Ca = 0.0018$. In the experiment, non-wetting phase fluid injection was stopped after a non-wetting phase pathway formed along the flow direction. During the wetting phase fluid injection, non-wetting phase fluids continuously snapped to form droplets distributed along the flow direction in the pore structure and microchannels. At low inlet capillary numbers, non-wetting phase fluids were more likely to have snap-off events (Tian et al. 2020; Li et al. 2021), resulting in more non-wetting phase droplets. These droplets were mainly distributed in the pore structure and at the microchannel entrance because the capillary force on them acts as a resistance. The inertial force was insufficient to overcome the capillary pressure to dislodge the droplets remaining upstream of the pore structure and microchannel, which later formed the non-wetting phase fluid residuals in the pore network structure (Ning et al. 2021).

Figure 9c shows the non-wetting phase residual distribution diagram for inlet $Ca = 0.024$. Non-wetting phase residual droplets were evenly distributed along the flow direction, but the final residuals were significantly smaller than for inlet $Ca = 0.0018$. At high inlet capillary numbers, droplets generated by non-wetting phase fluid snap-off events were more likely to break up and flow out of the pore network structure under the action of the local flow field. They were eventually distributed in the small pores and distal structures far from the flow direction. Increasing the inlet capillary number could significantly reduce non-wetting phase residuals in the pore network structure.

Fluid viscosity is an essential factor in the droplet breakup process and an important factor affecting the distribution of non-wetting phase residuals in the pore network structure (Wang et al. 2014; Bai et al. 2016; Liu et al. 2019; Esmaeili et al. 2020). Figure 10a shows that the distribution of non-wetting phase residuals was analyzed for different two-phase viscosity ratios. Low-viscosity non-wetting phase fluids easily broke up to form smaller droplets, while high-viscosity non-wetting phase fluids were likely to form larger droplets (Nie et al. 2008; Singh et al. 2019; Li et al. 2022). When inlet $Ca \approx 10^{-3}$ and the two-phase viscosity ratio $k = 0.08$, more than 75% of the non-wetting phase droplets remaining in the pore network structure occupied areas between 2×10^6 μm^2 and 10×10^6 μm^2 after the displacement process. About 12% of the residual non-wetting phase droplets occupied areas larger than 12×10^6 μm^2. For the same inlet capillary number and a two-phase viscosity ratio $k = 10.4$, more than 50% of non-wetting droplets remaining in the pore network structure had areas between 12×10^6 μm^2 and 22×10^6 μm^2, and only about 30% of the total droplets were had areas between 2×10^6 μm^2 and 10×10^6 μm^2 after the displacement process.

Comparing the distribution of non-wetting phase residuals in Fig. 10b and c shows that the high-viscosity non-wetting phase fluids eventually produced more residuals. Non-wetting phase fluids with high viscosity are more challenging to move. When the viscosity is high, the driving force has difficulty overcoming the surface constraint under the local flow field conditions. It wasn't easy to reduce the droplet size by initiating the snap-off events so that the droplet could flow out of the pore structure (Nie et al. 2008; Singh et al. 2019; Li et al. 2022). The non-wetting phase fluid residuals in the pore network structure were finally formed in the subsequent wetting phase fluid displacement process.

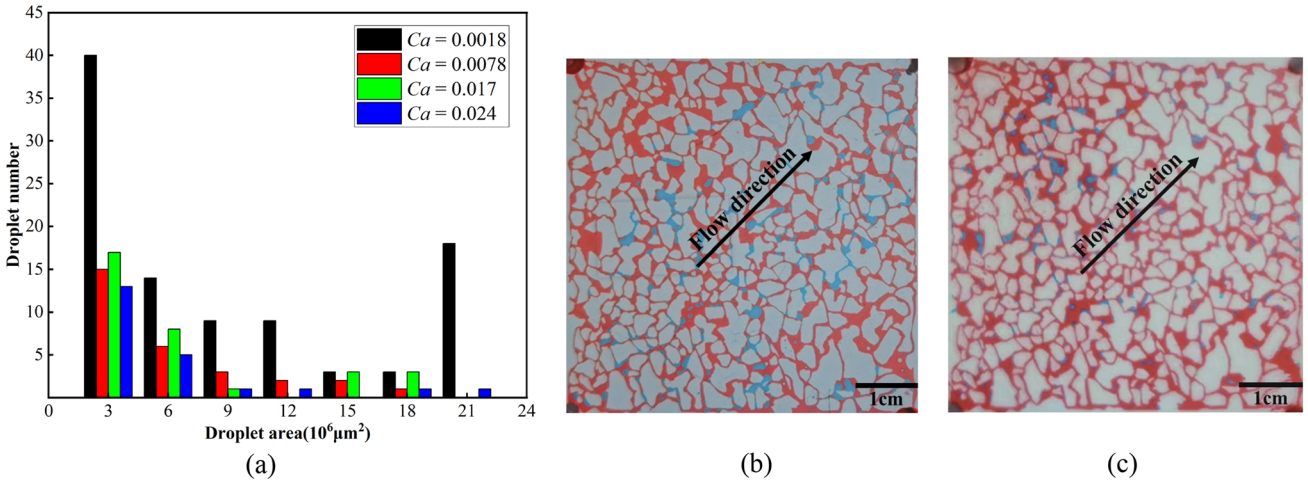

Fig. 10 Distribution diagrams of the non-wetting phase residuals in the displacement experiment. **a** is a statistical diagram of the residual droplets in the non-wetting phase for different viscosity ratios. Experiments were set up with materials M1-M4. **b** and **c** are the experimental diagrams of the non-wetting phase residual distribution at the viscosity ratio condition of $k=10.4$ and $k=0.08$, respectively. The red, blue and white parts represent the wetting phase fluid, non-wetting phase fluid and the PDMS substrates, respectively

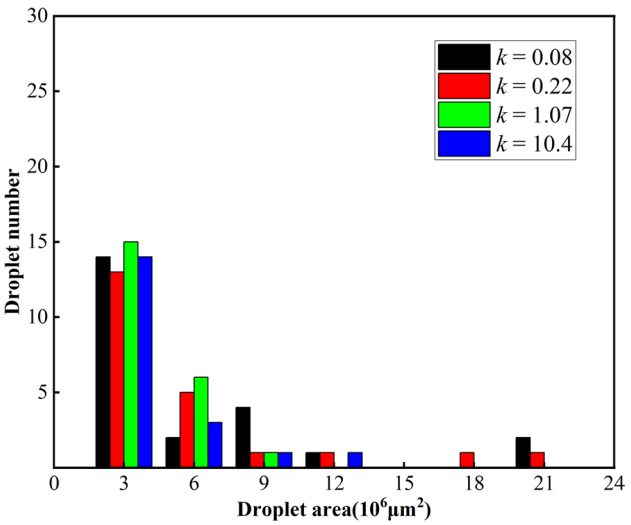

Fig. 11 Statistical diagram of the residual droplets in the non-wetting phase for different viscosity ratios. Experiments were set up with materials M1–M4 for inlet capillary number $Ca=0.024$

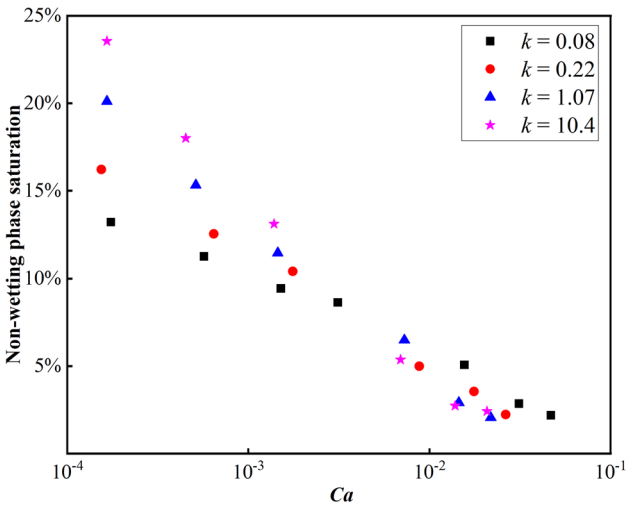

Fig. 12 Diagram of non-wetting phase saturation for different displacement conditions. The abscissa and ordinate are the capillary inlet number and non-wetting phase saturation, respectively

Non-wetting phase residuals in the pore network structure can be reduced by increasing the inlet capillary number and reducing the viscosity ratio. As shown in Fig. 11 at inlet $Ca=0.024$ and $k=0.08$, there were fewer non-wetting phase residuals in the pore network structure, and the droplets were mainly smaller than 10×10^6 μm^2, significantly reducing the non-wetting phase saturation in the pore network structure after the displacement process.

The non-wetting phase residuals can be reduced by adjusting the non-wetting phase fluids' snap-off events. As shown in Fig. 12 for the two-phase fluid system with different viscosity ratios, as the inlet wetting phase flow rate increased, the non-wetting phase fluid saturation decreased with increasing inlet capillary number. As the inlet capillary number rised, the capillary number of the local flow field also increased, reducing the non-wetting phase fluid snap-off events (Pak et al. 2015; Singh et al. 2017). For different viscosity ratio fluids with the same inlet capillary number, especially $Ca<10^{-2}$, non-wetting phase fluid with higher viscosity caused more residual saturation. Where $Ca>10^{-2}$, the difference in residual saturation caused by two-phase fluids with different viscosity ratios was unclear. The driving force generated by the increase of inlet velocity significantly

reduced the non-wetting phase fluid residuals along the flow direction, and the influence of viscosity on the non-wetting phase residuals became smaller (Rezaei et al. 2018; Zhang and Wang 2022).

For inlet $Ca = 0.031$ and $k = 0.08$, non-wetting phase saturation in the pore network structure decreased to 2.4% after displacement. Increasing the flow rate of two-phase fluids with different viscosity ratios reduced the non-wetting phase fluid saturation in the pore network. For a two-phase fluid with a fixed inlet flow rate and high snap-off events at inlet $Ca \approx 10^{-3}$, a higher two-phase viscosity ratio corresponded to a higher non-wetting phase saturation in the pore network. For the low snap-off events at inlet $Ca > 10^{-2}$, the viscosity ratio had little effect on non-wetting phase saturation in the pore network, which is below 5% for different flow conditions.

A comparison of the statistical diagrams of the residual droplets in Figs. 9a, 10a, and 11 indicates that the non-wetting phase fluid snap-off events could be reduced by increasing the viscosity of the displacement fluids, reducing the surface tension coefficient of the two phases, and increasing the injection flow rate of the displacement fluids, thereby reducing the non-wetting phase saturation. At the same time, because of the complex structure of real rock cores, there were small pore structures and terminal structures in porous media conducive to trapping non-wetting phase fluids. It was difficult to displace non-wetting phase fluids completely, but the non-wetting phase saturation could be minimized by adjusting the flow parameters.

5 Conclusions

This paper describes two-phase fluid displacement experiments on a PDMS chip with a two-dimensional heterogeneous pore network structure. The influence of non-wetting phase fluid snap-off events on the flow was analyzed based on displacement experiment results for non-wetting phase residuals. The results provide the details of the microscopic phenomenon caused by snap-off events, the non-wetting phase snap-off behavior in the pore network structure, and the residual distribution. The main conclusions of this paper are as follows:

(1) Non-wetting phase fluid snap-off events are the most common microscopic phenomenon in porous media two-phase flow processes. Although these snap-off events help free the trapped non-wetting phase in the microchannels, high-frequency snap-off events are the main reason for trapping the non-wetting phase during displacement, eventually leading to residuals.
(2) At an inlet capillary number $Ca \approx 10^{-3}$ ($Ca = 0.0018$), more snap-off events occurred in the non-wetting phase, and more non-wetting phase residuals were formed. The snap-off events were the primary mechanism for non-wetting phase trapping. As the inlet capillary number reached $Ca \approx 10^{-2}$ ($Ca = 0.017$), the number of non-wetting phase droplets increased and then decreased. At a certain flow rate, a larger two-phase viscosity ratio resulted in fewer non-wetting phase droplets generated during the displacement process. Non-wetting phase fluids with high viscosity were more difficult to snap.
(3) The influence of different viscosities on the non-wetting phase residual distribution shows that non-wetting phase fluids with low viscosity can easily form tiny droplets, while non-wetting phase fluids with high viscosity form large droplets more easily.
(4) Increasing the inlet capillary number reduces the non-wetting phase fluid saturation in the pore network for the two-phase fluid at different viscosity ratios. A higher two-phase viscosity ratio causes higher non-wetting phase saturation in the pore network at a certain inlet flow rate. Non-wetting phase fluids with high viscosities are more challenging to move because the driving force cannot easily overcome the surface constraint for the local flow field condition and because it is difficult to start snap-off events to reduce the droplet size to move some of the trapped droplets out of the pore structure. The non-wetting phase fluid snap-off frequency in the pore network structure can be reduced to lower the non-wetting phase fluid saturation by increasing the displacement fluid viscosity, reducing the surface tension coefficient between the two phases, and increasing the flow rate.

Author contributions RL and ZL: were involved in the experiments and wrote the main manuscript text. ZG and WL: contributed to the writing—reviewing and editing. GZ: helped with the writing—review and editing, and supervision. JS: contributed to the conceptualisation, methodology, writing-reviewing and editing, and supervision. All authors reviewed the manuscript.

Funding This work was supported by the Key Research and Development Program of Shaanxi (Program No. 2023-YBSF-218, 2021GXLH-Z-071) and the National Natural Science Foundation of China (No. 12072256).

Availability of data and materials The data and materials are available from the corresponding author on reasonable request.

Declarations

Conflict of interest The authors declare that they have no competing interests as defined by Springer, or other interests that might be perceived to influence the results and/or discussion reported in this paper.

Ethical approval Not applicable.

References

Alhosani A, Scanziani A, Lin Q et al (2020) Dynamics of water injection in an oil-wet reservoir rock at subsurface conditions: Invasion patterns and pore-filling events. Phys Rev E 102:23110. https://doi.org/10.1103/PhysRevE.102.023110

Alyafei N, Blunt MJ (2016) The effect of wettability on capillary trapping in carbonates. Adv Water Resour 90:36–50. https://doi.org/10.1016/j.advwatres.2016.02.001

Andrew M, Menke H, Blunt MJ, Bijeljic B (2015) The imaging of dynamic multi-phase fluid flow using synchrotron-based X-ray microtomography at reservoir conditions. Transp Porous Media 110:1–24. https://doi.org/10.1007/s11242-015-0553-2

Ayirala SC, Al-Saleh SH, Al-Yousef AA (2018) Microscopic scale interactions of water ions at crude oil/water interface and their impact on oil mobilisation in advanced water flooding. J Pet Sci Eng 163:640–649. https://doi.org/10.1016/j.petrol.2017.09.054

Bai L, Fu Y, Zhao S, Cheng Y (2016) Droplet formation in a microfluidic T-junction involving highly viscous fluid systems. Chem Eng Sci 145:141–148. https://doi.org/10.1016/j.ces.2016.02.013

Beresnev IA, Li W, Vigil RD (2009) Condition for breakup of non-wetting fluids in sinusoidally constricted capillary channels. Transp Porous Media 80:581–604. https://doi.org/10.1007/s11242-009-9381-6

Berg S, Rücker M, Ott H et al (2016) Connected pathway relative permeability from pore-scale imaging of imbibition. Adv Water Resour 90:24–35. https://doi.org/10.1016/j.advwatres.2016.01.010

Blunt MJ (1998) Physically-based network modeling of multi-phase flow in intermediate-wet porous media. J Pet Sci Eng 20:117–125. https://doi.org/10.1016/S0920-4105(98)00010-2

Buchgraber M, Al-Dossary M, Ross CM, Kovscek AR (2012) Creation of a dual-porosity micromodel for pore-level visualisation of multi-phase flow. J Pet Sci Eng 86–87:27–38. https://doi.org/10.1016/j.petrol.2012.03.012

Chen M, Yortsos YC, Rossen WR (2005) Insights on foam generation in porous media from pore-network studies. Colloids Surfaces A Physicochem Eng Asp 256:181–189. https://doi.org/10.1016/j.colsurfa.2005.01.020

Cubaud T, Mason TG (2008) Capillary threads and viscous droplets in square microchannels. Phys Fluids. https://doi.org/10.1063/1.2911716

Cui J, Zhang Z, Liu G et al (2022) Breakthrough pressure anisotropy and intra-source migration model of crude oil in shale. Mar Pet Geol 135:105433. https://doi.org/10.1016/j.marpetgeo.2021.105433

Datta SS, Ramakrishnan TS, Weitz DA (2014) Mobilisation of a trapped non-wetting fluid from a three-dimensional porous medium. Phys Fluids. https://doi.org/10.1063/1.4866641

Esmaeili S, Modaresghazani J, Sarma H et al (2020) Effect of temperature on relative permeability—role of viscosity ratio. Fuel 278:118318. https://doi.org/10.1016/j.fuel.2020.118318

Garstecki P, Stone HA, Whitesides GM (2005) Mechanism for flow-rate controlled breakup in confined geometries: a route to monodisperse emulsions. Phys Rev Lett 94:1–4. https://doi.org/10.1103/PhysRevLett.94.164501

Ghanbarian B, Hunt AG, Ewing RP, Sahimi M (2013) Tortuosity in porous media: a critical review. Soil Sci Soc Am J 77:1461–1477. https://doi.org/10.2136/sssaj2012.0435

Hammond PS (1983) Nonlinear adjustment of a thin annular film of viscous fluid surrounding a thread of another within a circular cylindrical pipe. J Fluid Mech 137:363–384. https://doi.org/10.1017/S0022112083002451

Heydari-Farsani E, Neilson JE, Alsop GI, Hamidi H (2020) The effect of rock type on natural water flooding and residual oil saturation below free water level and oil water contact: a case study from the Middle East. J Pet Sci Eng 193:107392. https://doi.org/10.1016/j.petrol.2020.107392

Jin BJ, Kim YW, Lee Y, Yoo JY (2010) Droplet merging in a straight microchannel using droplet size or viscosity difference. J Micromech Microeng. https://doi.org/10.1088/0960-1317/20/3/035003

Joekar-Niasar V, Hassanizadeh SM (2012) Analysis of fundamentals of two-phase flow in porous media using dynamic pore-network models: a review. Crit Rev Environ Sci Technol 42:1895–1976. https://doi.org/10.1080/10643389.2011.574101

Lenormand R, Zarcone C, Sarr A (1983) Mechanisms of the displacement of one fluid by another in a network of capillary ducts. J Fluid Mech 135:337–353. https://doi.org/10.1017/S0022112083003110

Li Y, Blois G, Kazemifar F, Christensen KT (2019) High-speed quantification of pore-scale multi-phase flow of water and supercritical CO2 in 2-D heterogeneous porous micromodels: flow regimes and interface dynamics. Water Resour Res 55:3758–3779. https://doi.org/10.1029/2018WR024635

Li Z, Gu Z, Li R et al (2021) Investigation on droplet dynamic snap-off process in a short, abrupt constriction. Chem Eng Sci 235:116496. https://doi.org/10.1016/j.ces.2021.116496

Li Z, Gu Z, Li R et al (2022) A geometrical criterion for the dynamic snap-off event of a non-wetting droplet in a rectangular pore-throat microchannel. Phys Fluids. https://doi.org/10.1063/5.0087523

Liang T, Xu K, Lu J et al (2020) Evaluating the performance of surfactants in enhancing flowback and permeability after hydraulic fracturing through a microfluidic model. SPE J 25:268–287. https://doi.org/10.2118/199346-PA

Liu Z, Li M, Pang Y et al (2019) Flow characteristics inside droplets moving in a curved microchannel with rectangular section. Phys Fluids. https://doi.org/10.1063/1.5080373

Mahdavi S, James LA (2019) Micro and macro analysis of carbonated water injection (CWI) in homogeneous and heterogeneous porous media. Fuel 257:115916. https://doi.org/10.1016/j.fuel.2019.115916

Mehmani A, Kelly S, Torres-Verdín C, Balhoff M (2019) Residual oil saturation following gas injection in sandstones: microfluidic quantification of the impact of pore-scale surface roughness. Fuel 251:147–161. https://doi.org/10.1016/j.fuel.2019.02.118

Nie Z, Seo MS, Xu S et al (2008) Emulsification in a microfluidic flow-focusing device: effect of the viscosities of the liquids. Microfluid Nanofluidics 5:585–594. https://doi.org/10.1007/s10404-008-0271-y

Ning T, Xi M, Hu B et al (2021) Effect of viscosity action and capillarity on pore-scale oil–water flowing behaviors in a low-permeability sandstone waterflood. Energies. https://doi.org/10.3390/en14248200

Osei-Bonsu K, Grassia P, Shokri N (2018) Effects of pore geometry on flowing foam dynamics in 3D-printed porous media. Transp Porous Media 124:903–917. https://doi.org/10.1007/s11242-018-1103-5

Pak T, Butler IB, Geiger S et al (2015) Droplet fragmentation: 3D imaging of a previously unidentified pore-scale process during multi-phase flow in porous media. Proc Natl Acad Sci U S A 112:1947–1952. https://doi.org/10.1073/pnas.1420202112

Peña TJ, Carvalho MS, Alvarado V (2009) Snap-off of a liquid drop immersed in another liquid flowing through a constricted capillary. AIChE J 55:1993–1999. https://doi.org/10.1002/aic

Perazzo A, Tomaiuolo G, Preziosi V, Guido S (2018) Emulsions in porous media: from single droplet behavior to applications for oil

recovery. Adv Colloid Interface Sci 256:305–325. https://doi.org/10.1016/j.cis.2018.03.002
Rezaei N, Zendehboudi S, Chatzis I, Lohi A (2018) Combined benefits of capillary barrier and injection pressure control to improve fluid recovery at breakthrough upon gas injection: an experimental study. Fuel 211:638–648. https://doi.org/10.1016/j.fuel.2017.09.048
Riazi M, Sohrabi M, Bernstone C et al (2011) Visualisation of mechanisms involved in CO2 injection and storage in hydrocarbon reservoirsand water-bearing aquifers. Chem Eng Res Des 89:1827–1840. https://doi.org/10.1016/j.cherd.2011.03.009
Rogers JA, Nuzzo RG (2005) Recent progress in soft lithography. Mater Today 8:50–56. https://doi.org/10.1016/S1369-7021(05)00702-9
Roman S, Abu-Al-Saud MO, Tokunaga T et al (2017) Measurements and simulation of liquid films during drainage displacements and snap-off in constricted capillary tubes. J Colloid Interface Sci 507:279–289. https://doi.org/10.1016/j.jcis.2017.07.092
Rossen WR (2000) Snap-off in constricted tubes and porous media. Colloids Surfaces A Physicochem Eng Asp 166:101–107. https://doi.org/10.1016/S0927-7757(99)00408-2
Ruspini LC, Farokhpoor R, Øren PE (2017) Pore-scale modeling of capillary trapping in water-wet porous media: a new cooperative pore-body filling model. Adv Water Resour 108:1–14. https://doi.org/10.1016/j.advwatres.2017.07.008
Singh K, Bijeljic B, Blunt MJ (2016) Imaging of oil layers, curvature and contact angle in a mixed- wet and a water-wet carbonate rock. Water Resour Res 52:1716–1728. https://doi.org/10.1111/j.1752-1688.1969.tb04897.x
Singh K, Menke H, Andrew M et al (2017) Dynamics of snap-off and pore-filling events during two-phase fluid flow in permeable media. Sci. Rep. 7(1):5192
Singh K, Jung M, Brinkmann M, Seemann R (2019) Capillary-dominated fluid displacement in porous media. Annu Rev Fluid Mech 51:429–449. https://doi.org/10.1146/annurev-fluid-010518-040342
Song W, Hatzignatiou DG (2022) On the reduction of the residual oil saturation through the injection of polymer and nanoparticle solutions. J Pet Sci Eng 208:109430. https://doi.org/10.1016/j.petrol.2021.109430
Tian J, Kang Y, Xi Z et al (2020) Real-time visualisation and investigation of dynamic gas snap-off mechanisms in 2-D micro channels. Fuel 279:118232. https://doi.org/10.1016/j.fuel.2020.118232
Wang X, Wang K, Riaud A et al (2014) Experimental study of liquid/liquid second-dispersion process in constrictive microchannels. Chem Eng J 254:443–451. https://doi.org/10.1016/j.cej.2014.05.135
Xu K, Liang T, Zhu P et al (2017) A 2.5-D glass micromodel for investigation of multi-phase flow in porous media. Lab Chip 17:640–646. https://doi.org/10.1039/c6lc01476c
Yun W, Kovscek AR (2015) Microvisual investigation of polymer retention on the homogeneous pore network of a micromodel. J Pet Sci Eng 128:115–127. https://doi.org/10.1016/j.petrol.2015.02.004
Yun W, Ross CM, Roman S, Kovscek AR (2017) Creation of a dual-porosity and dual-depth micromodel for the study of multi-phase flow in complex porous media. Lab Chip 17:1462–1474. https://doi.org/10.1039/c6lc01343k
Zhang C, Wang M (2022) A critical review of breakthrough pressure for tight rocks and relevant factors. J Nat Gas Sci Eng 100:104456. https://doi.org/10.1016/j.jngse.2022.104456